CLINICAL SCIENCE

Clinically low-risk prostate cancer: evaluation with transrectal doppler ultrasound and functional magnetic resonance imaging

Maria Inês Novis,[I] Ronaldo Hueb Baroni,[I] Luciana Mendes de Oliveira Cerri,[I] Romulo Loss Mattedi,[I] Carlos Alberto Buchpiguel[II]

[I]Faculdade de Medicina da Universidade de São Paulo - Hospital das Clínicas, São Paulo, Brazil. [II]Radiology, Faculdade de Medicina da Universidade de São Paulo - Hospital das Clínicas, São Paulo, Brazil.

OBJECTIVES: To evaluate transrectal ultrasound, amplitude Doppler ultrasound, conventional T_2-weighted magnetic resonance imaging, spectroscopy and dynamic contrast-enhanced magnetic resonance imaging in localizing and locally staging low-risk prostate cancer.

INTRODUCTION: Prostate cancer has been diagnosed at earlier stages and the most accepted classification for low-risk prostate cancer is based on clinical stage T1c or T2a, Gleason score $\leq$6, and prostate-specific antigen (PSA) $\leq$10 ng/ml.

METHODS: From 2005 to 2006, magnetic resonance imaging was performed in 42 patients, and transrectal ultrasound in 26 of these patients. Seven patients were excluded from the study. Mean patient age was 64.94 years and mean serum PSA was 6.05 ng/ml. The examinations were analyzed for tumor identification and location in prostate sextants, detection of extracapsular extension, and seminal vesicle invasion, using surgical pathology findings as the gold standard.

RESULTS: Sixteen patients (45.7%) had pathologically proven organ-confined disease, 11 (31.4%) had positive surgical margin, 8 (28.9%) had extracapsular extension, and 3 (8.6%) presented with extracapsular extension and seminal vesicle invasion. Sensitivity, specificity, positive predictive value (PPV), negative predictive value (NPV) and accuracy values for localizing low-risk prostate cancer were 53.1%, 48.3%, 63.4%, 37.8% and 51.3% for transrectal ultrasound; 70.4%, 36.2%, 65.1%, 42.0% and 57.7% for amplitude Doppler ultrasound; 71.5%, 58.9%, 76.6%, 52.4% and 67.1% for magnetic resonance imaging; 70.4%, 58.7%, 78.4%, 48.2% and 66.7% for magnetic resonance spectroscopy; 67.2%, 65.7%, 79.3%, 50.6% and 66.7% for dynamic contrast-enhanced magnetic resonance imaging, respectively. Sensitivity, specificity, PPV, NPV and accuracy values for detecting extracapsular extension were 33.3%, 92%, 14.3%, 97.2% and 89.7% for transrectal ultrasound and 50.0%, 77.6%, 13.7%, 95.6% and 75.7% for magnetic resonance imaging, respectively. For detecting seminal vesicle invasion, these values were 66.7%, 85.7%, 22.2%, 97.7% and 84.6% for transrectal ultrasound and 40.0%, 83.1%, 15.4%, 94.7% and 80.0% for magnetic resonance imaging.

CONCLUSION: Although preliminary, our results suggest that imaging modalities have limited usefulness in localizing and locally staging clinically low-risk prostate cancer.

KEYWORDS: Prostatic neoplasm; Cancer staging; Magnetic Resonance Imaging; Magnetic Resonance Spectroscopy; Ultrasonography; Doppler Ultrasound.

Novis MI, Baroni RH, Cerri LMO, Mattedi RL, Buchpiguel CA. Clinically low-risk prostate cancer: evaluation with transrectal doppler ultrasound and functional magnetic resonance imaging. Clinics. 2011;66(1):27-34.

Received for publication on August 22, 2010; **First review completed on** September 16, 2010; **Accepted for publication on** October 3, 2010

E-mail: inesnovis@hotmail.com

Tel.: 55 11 3069-6000

INTRODUCTION

The widespread use of prostate-specific antigen (PSA) testing, associated with both improved biopsy techniques for diagnosis and public awareness has led to an increase in prostate cancer detection in recent decades.[1] Moreover, this phenomenon has been accompanied by a decrease in the mortality rate related to prostate cancer in many countries, probably because it is being detected at earlier stages, when tumors are often small and of low aggressiveness.[2]

One of the most important current challenges in prostate cancer is to distinguish patients with clinically relevant disease, who may benefit from early radical treatment, from those with more indolent disease, avoiding overtreatment

and consequent morbidity. The classification of prostate cancer into high-, intermediate-, and low-risk disease is an attempt to stratify patients' management focusing on their individual needs.[3]

A recent published study has clearly demonstrated this downward stage migration, analyzing data from over 8000 men diagnosed with prostate cancer. In the last two decades, the rate of detection of low-risk prostate cancer has shown an increase, ranging from 28% to 45.3%.[4]

One of the most accepted classifications for low-risk prostate cancer was proposed by D'Amico et al.[5] more than 10 years ago, and is based on prognostic factors that reduce the probability of post-therapy PSA failure (<25% at 5 years). Low-risk prostate cancer was defined as clinical T-stage T1c or T2a (undetected or limited to one lobe on digital rectal examination), Gleason score ≤6, and PSA ≤10 ng/ml.

Nevertheless, this definition of low-risk cancer is based on pretreatment clinical assessment and can represent a significant or insignificant tumor on surgical pathology, with widely different prognosis. The pathological definition of insignificant tumor consists in an organ-confined cancer with a total volume ≤0.5 ml, and no poorly differentiated components (Gleason ≥4) on surgical histopathology.[6]

There is still no reliable non-invasive marker to predict individual profiles in the low-risk category of prostate cancer. Imaging is gaining widespread acceptance, especially magnetic resonance imaging (MRI), which provides an excellent zonal anatomy resolution, besides functional and metabolic information. Although the importance of these methods for tumor diagnosis and location, assessment of tumor aggressiveness, treatment planning, and follow-up have been well studied, the potential of imaging in the evaluation of low-risk prostate cancer still needs further investigation.[7]

The aim of this study was to evaluate transrectal ultrasound (TRUS), amplitude Doppler ultrasound (ADUS), conventional MRI, magnetic resonance spectroscopy (MRS) and dynamic contrast-enhanced imaging (DCE-MRI) in localizing and locally staging low-risk prostate cancer, using surgical pathology findings as gold standard.

MATERIALS AND METHODS

Patient characteristics and demographics

Institutional Review Board approval and written informed consent from all patients were obtained for this prospective study. Patient data were collected from January 2005 to December 2006. Forty-two patients referred from the Urology Department met the following inclusion criteria: a) ultrasound-guided biopsy-proven prostate cancer, b) no prior history of hormonal blockade, c) candidate for retropubic prostatectomy, d) clinical T-stage T1c–T2a, e) biopsy Gleason score ≤6 and f) PSA ≤10 ng/ml. MRI examination was performed with a minimal interval of 21 days after prostate biopsy to minimize hemorrhagic artifacts. Serum level of PSA, Gleason grade at biopsy, and digital rectal examination results were collected from the medical records.

Of these 42 patients, 3 were excluded from the study because prostatectomy had been performed at other institutions, 3 were referred to other therapy due to high surgical risk and 1 died from non-related causes before surgery.

The final group consisted of 35 patients who underwent MRI examination before surgery, 26 of whom were also submitted to TRUS. The other nine patients declined to undergo ultrasound after their initial enrollment.

The mean patient age was 64.94 years (range 50–77 years), mean serum level of PSA was 6.05 ng/ml (range 2.6–10.0 ng/ml). Two patients (5.7%) had a total Gleason biopsy score of 5, and the remaining 33 (94.3%) had a total Gleason biopsy score of 6. The mean intervals between imaging examinations and surgery were 49.34 days for MRI and 48.35 for TRUS (range 4–145 days).

Conventional MRI technique

Endorectal MRI was performed with a 1.5-T MRI system (Signa; GE Medical Systems, Milwaukee, WI, USA), using a pelvic phased-array coil (Torso PA; GE Medical Systems) in combination with a commercially available balloon-covered expandable endorectal coil (Endo ATD; Medrad, Pittsburgh, PA, USA) for signal reception. The endorectal coil was inflated with 60 ml of liquid perfluorocarbon to reduce the high magnetic field susceptibility at the air–tissue interface and improve the quality of MR spectroscopic imaging data.

T_1-weighted (T1W) axial fast multiplanar spoiled gradient-echo (FMSPGR) images from the pelvis were obtained from the aortic bifurcation to the symphysis pubis with the following parameters: repetition time (TR)/echo time (TE), 200/4.2; flip angle, 90°; slice thickness, 7 mm; interslice gap, 1 mm; field of view (FOV), 30 cm; matrix, 256 × 192; frequency direction, transverse (right to left); and number of excitations (NEX), 1. Thin-section, high spatial resolution axial, sagittal and coronal T_2-weighted (T2W) fast spin-echo images from below the prostate apex to above the seminal vesicles (SSVV) were obtained with the following parameters: TR/TE, 4000/150; slice thickness, 3 mm; interslice gap, 0–1 mm; FOV, 14 cm; matrix, 256 × 192; frequency direction, anteroposterior (AP) (for sagittal and axial images), no-phase-wrap (to avoid phase oversampling); and NEX, 3.

MRI spectroscopic technique

After reviewing the transverse T2W images, a spectroscopic imaging volume was selected to maximize coverage of the whole prostate. Three-dimensional MRS data were acquired by using point-resolved spatially localized spectroscopy (PRESS), which was optimized for quantitative detection of both choline and citrate. Water and lipid suppression was achieved by using the spectral-spatial pulses capable of both volume selection and frequency selection. Outer voxel saturation pulses were also used to eliminate signals from adjacent tissues. Data sets were acquired as 16 × 8 × 8 phase-encoded spectral arrays (1024 voxels; nominal spatial resolution, 0.34 cm^3; 1000/130; acquisition time, 17 min).

Dynamic contrast-enhanced MRI technique

High spatial resolution DCE-MRI was performed with application of a fast three-dimensional T1W spoiled gradient-echo sequence with a voxel size of 1.79 mm^3 (0.95 × 0.63 × 3 mm), as described in a recent study.[8] Seven three-dimensional data sets, two before and five after contrast agent administration, were acquired under a 1 min and 35 s temporal resolution and a total duration of 11 min

and 8 s. The MR contrast agent, gadopentetate dimeglumine (Magnevist, Schering), was injected as a bolus at a dose of 0.1 mmol per kilogram of body weight at 2 ml/s starting 5–7 s before the end of the second acquisition, followed by a 20-ml saline flush.

MRI interpretation

All MRI data were analyzed by the same radiologist, with 8 years' experience in prostate MRI. The reader was not completely blinded since he was aware that the patient had biopsy-proven prostate cancer, but unaware of any other clinical or laboratory data. Tumor identification was defined by a conspicuous hypointense nodule or an ill-defined low-signal area on T2W images, with tumor location being determined within prostate sextants. The diagnostic criteria used to determine the extracapsular extension (ECE) included at least one of the following: irregular capsular bulge, direct extension of low signal intensity tumor into periprostatic fat and/or obliteration of the rectoprostatic angle.[9] Seminal vesicle invasion (SVI) was defined as loss of the normal SSVV architecture, focal or diffuse areas of low signal intensity within the SSVV and/or direct extension of the low signal intensity of tumor from the base of the prostate to the SSVV.[10]

MRS data were digitally processed by using Functool software (Advantage workstation, GE Healthcare), overlaid on the corresponding transverse T2W images. Signal-to-noise ratios were automatically calculated as the ratio between citrate or choline peak amplitude and the standard deviation of the noise over the 0.53–0.96 ppm range. Voxels considered suitable had signal-to-noise ratio ≥ 2 (ranging from 2 to 8). Ten patients were excluded from spectral analysis because they presented voxels of insufficient spectral quality, signal-to-noise <2 or were spectroscopically contaminated because of insufficient water or fat suppression. Suitable spectroscopic voxels were analyzed by a quantitative and qualitative approach: positivity was determined by a choline plus creatine-to-citrate ratio ≥ 0.7 and by an elevation of the choline and reduction of the citrate peaks, such that these peaks were of similar height or the choline one was higher.[11] One positive voxel defined tumor presence within its sextant, independently of coexisting abnormal T2W findings.

DCE-MRI was processed using the three-timepoint model to analyze the time evolution of contrast enhancement.[8] A positive pattern was defined as increased wash-in followed by a decreasing curve characterizing washout, and at least one positive ROI within the sextant was sufficient to define its positivity. Dynamic analysis was performed independently of the T2W images. Steady state and continuous enhancement patterns were considered negative for cancer.

Post-biopsy hemorrhage signs within the prostate on T1W images were identified in three patients without significant implications for MRI analysis.

Transrectal ultrasound technique and interpretation

All the TRUS examinations were performed and interpreted by the same radiologist, with 15 years' experience in prostate ultrasound, who was blinded to all patient information except for biopsy-proven prostate cancer. All the examinations were performed in a General Electric Logiq 9 equipment (GE Medical Systems) with a probe frequency of 7.5 MHz. TRUS gray-scale findings for tumor identification were defined as the presence of a definite hypoechoic nodule or an area of heterogeneous echotexture; tumor location was determined within the prostate sextants. The assessment of the ECE depended on identification of an irregular bulge in the prostate contour, direct extension of solid tissue in the periprostatic fat and/or rectoprostatic angle obliteration. SVI was characterized by thickening and hypoechogenicity of the SSVV. ADUS was then performed independently of gray-scale findings. Doppler gain was set as high as possible without background noise. The amount of flow within each sextant was determined on the basis of visual inspection of the pixel density, and hypervascularity was defined as the presence of higher than normal blood flow in each distinct sextant of the prostate, with irregular, tortuous, and/or disorganized vessels, as well as areas of vascular asymmetry being interpreted as suspicious for cancer.

Histopathological results

After preparation, axial step sections were obtained at 3- to 4-mm intervals, in planes closely paralleling the MR images, and stained with hematoxylin and eosin (HE). Tumor presence and Gleason grade were recorded for each sextant, as well as the presence of ECE and surgical positive margins. SVI was recorded by side of involvement. The final classification was performed using TNM staging classification and the Gleason score and used as the reference standard.

Statistical analysis

The sensitivity, specificity, accuracy, PPVs and NPVs were calculated for tumor identification in the different techniques evaluated: TRUS, ADUS, MRI, MRS and DCE-MRI. Sensitivity, specificity, accuracy, PPVs and NPVs were also calculated for ECE and SVI detection by TRUS and MRI. The kappa index of agreement was calculated for each technique. All these analyses utilized histopathological results as the gold standard, according to sextant localization.

RESULTS

From the 35 patients with clinically defined low-risk prostate cancer who underwent radical prostatectomy, only 16 (45.7%) had pathologically proven organ-confined disease; clinical and histopathological variables are demonstrated in Tables 1 and 2, respectively. Both clinical stage and biopsy Gleason grade underestimated the surgical findings. Positive surgical margins were found in 11 patients (31.4%), ECE was detected in eight patients (28.9%); three of them (8.6%) also presented with SVI.

The performance of the different imaging methods evaluated in localizing low-risk prostate cancer is demonstrated in Table 3. Although TRUS presented slight

Table 1 - Distribution of preoperative clinical variables.

PSA level (ng/ml) (mean $\pm$ SD)	6.05 $\pm$ 2.16
Biopsy Gleason grade	
5	2 (5.7%)
6	33 (94.3%)
Clinical stage	
T1c	29 (82.9%)
T2a	6 (17.1%)

Table 2 - Distribution of histopathological variables (post-prostatectomy specimen).

Gleason grade	
6 (3 + 3)	13 (37.1%)
7 (3 + 4)	18 (51.4%)*
7 (4 + 3)	03 (8.6%)†
8 (3 + 5)	01 (2.9%)
Histopathological stage	
pT2a	02 (5.7%)
pT2b	03 (8.6%)
pT2c	11 (31.4%)
pT2+ (positive surgical margins)	11 (31.4%)
pT3a (extracapsular extension)	08 (22.9%)
pT3b (seminal vesicle invasion)	03 (8.6%)

*4 of which had tertiary Gleason 5.
†1 of which had tertiary Gleason 5.

agreement with the histopathology based on the kappa index, the use of ADUS increases the sensitivity (from 53.1% to 70.4%; p 0.0187), with a discrete decrease in specificity (from 48.3% to 36.2%). MRI presented reasonable kappa index agreement, and the inclusion of MRS or DCE-MRI did not produce a significant improvement in the performance when compared with MRI sequence analysis (sensitivity values of 71.5% for MRI, 70.4% for MRS and 67.2% for DCE-MRI, $p>0.05$).

TRUS and MRI were also evaluated for detecting ECE, both demonstrating similar accuracies compared with the surgical pathology (kappa 0.15 and 0.12, respectively). The sensitivity, specificity, PPV, NPV and accuracy for detecting ECE were 33.3%, 92.0%, 14.3%, 97.2% and 89.7% for TRUS, and 50.0%, 77.6%, 13.7%, 95.6% and 75.7% for MRI, respectively (Table 4).

In the group under evaluation, only three patients (8.6%) presented with SVI, being unilateral in one patient and bilateral in the other two (Table 5). Although both methods showed high specificity, NPV, and accuracy (85.7%, 97.7% and 84.6% for TRUS and 83.1%, 94.7% and 80.0% for MRI), they lacked sensitivity and PPV.

Table 4 - Evaluation of TRUS and MRI in detecting ECE of low-risk prostate cancer.

	Sensitivity (%)	Specificity (%)	PPV (%)	NPV (%)	Accuracy (%)	kappa
TRUS	33.3	92.0	14.3	97.2	89.7	0.15
MRI	50.0	77.6	13.7	95.6	75.7	0.12

Table 5 - Evaluation of TRUS and MRI in detecting SVI of low-risk prostate cancer.

	Sensitivity (%)	Specificity (%)	PPV (%)	NPV (%)	Accuracy (%)	kappa
TRUS	66.7	85.7	22.2	97.7	84.6	0.27
MRI	40.0	83.1	15.4	94.7	80.0	0.13

DISCUSSION

There has been an increasing incidence of clinically defined low-risk prostate cancers in PSA-screened populations, for whom disease management remains controversial. There is no reliable method to distinguish patients who have indolent disease from those with progressive and life-threatening tumors within this low-risk group.[12]

Adverse pathologic features at surgery are defined as any of these criteria: tumor volume ≥0.5 ml, extraprostatic extension (EPE), positive surgical margins, or the presence of Gleason score >6,1. Based on this definition, all of our 35 patients with clinically defined low-risk prostate cancer had adverse pathologic findings: all of them presented tumor volume ≥0.5 ml, 8 patients had EPE (all of them with ECE and 3 also with SVI), 22 presented a Gleason score >6 and 11 had positive surgical margins. A recent meta-analysis reviewed 29 articles (1995–2006) that retrospectively examined outcomes in men with microfocal prostate cancer on biopsy, almost all of whom had low-risk disease according to the D'Amico classification, and up to 84% of them had adverse pathological findings at radical prostatectomy.[12] However, not all patients with adverse pathologic results have clinically significant disease.

The ability to determine the correct cancer location within the prostate and the number of sextants involved has important clinical value, because tumor volume is a relevant prognostic factor and also for considering the actual role of the local therapies. Huge heterogeneity exists in the available MRI literature, strongly affected by methodological and population variables, with cancer detection sensitivity varying between 37% and 90%.[13] Although large-volume cancers can be reasonably well detected by imaging, small lesions have been difficult to identify or measure accurately.[3] Also, aggressive tumors with higher Gleason scores present more evident architectural disarray on histology, probably improving their differentiation from the normal gland in imaging studies. In contrast, our difficulty in identifying many lesions in this study may be explained by the lower Gleason grades, represented by more differentiated cells that may be indistinguishable from the normal gland on imaging (Figures 1 and 2).

The results of several studies have suggested that MRS may provide additional useful information based on the metabolic changes associated with the disease, which might even precede morphological changes, improving assessment of tumor location, volume, staging, and estimation of aggressiveness.[14] However, a recently published prospective multicenter study that evaluated 110 patients with MRI and MRS demonstrated that the accuracy of combined MRI–MRS for sextant localization of prostate cancer in the peripheral zone is equal to that obtained by MRI alone.[15]

Table 3 - Evaluation of different imaging methods in localizing low-risk prostate cancer.

	Sensitivity (%)	Specificity (%)	PPV (%)	NPV (%)	Accuracy (%)	kappa
TRUS	53.1	48.3	63.4	37.8	51.3	0.01
ADUS	70.4	36.2	65.1	42.0	57.7	0.07
MRI	71.5	58.9	76.6	52.4	67.1	0.30
MRS	70.4	58.7	78.4	48.2	66.7	0.28
DCE-MRI	67.2	65.7	79.3	50.6	66.7	0.31

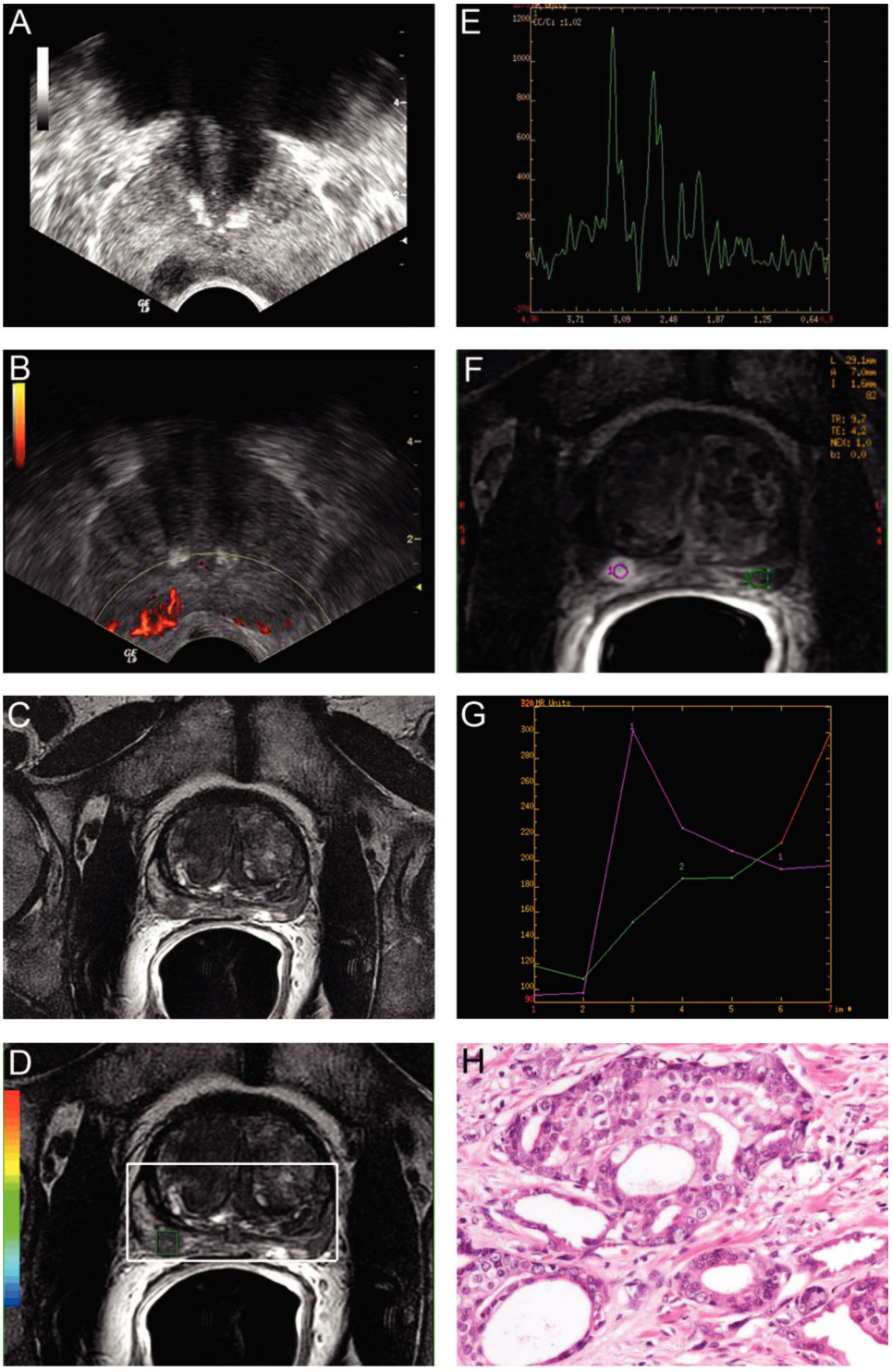

Figure 1 - 64-year-old man with prostate cancer (prostate specific antigen (PSA) level 5.2 ng/ml). (a) Transverse transrectal ultrasound (TRUS) demonstrates a hypoechoic nodule in the right mid-gland peripheral zone, hypervascularized in amplitude Doppler ultrasound (ADUS) (b). Transverse T2-weighted (T2W) magnetic resonance imaging (MRI) (c) shows a hypointense nodule in the right mid-gland. This voxel (d) and the corresponding amplitude times frequency spectroscopic graphic (e) shows reduced citrate and increased choline–creatine levels, suspicious for prostate cancer. Transverse T1W DCE-MRI (f) demonstrates increased vascularization in the nodule (pink region of interest (ROI)) and normal hypovascularized peripheral zone in the left mid-gland (green ROI), characterized on graphic (g) by washin followed by a decreasing washout curve and continuous enhancement patterns, respectively. Surgically confirmed adenocarcinoma Gleason score 7 (4 + 3) in the right mid-gland – HE 400× (h).

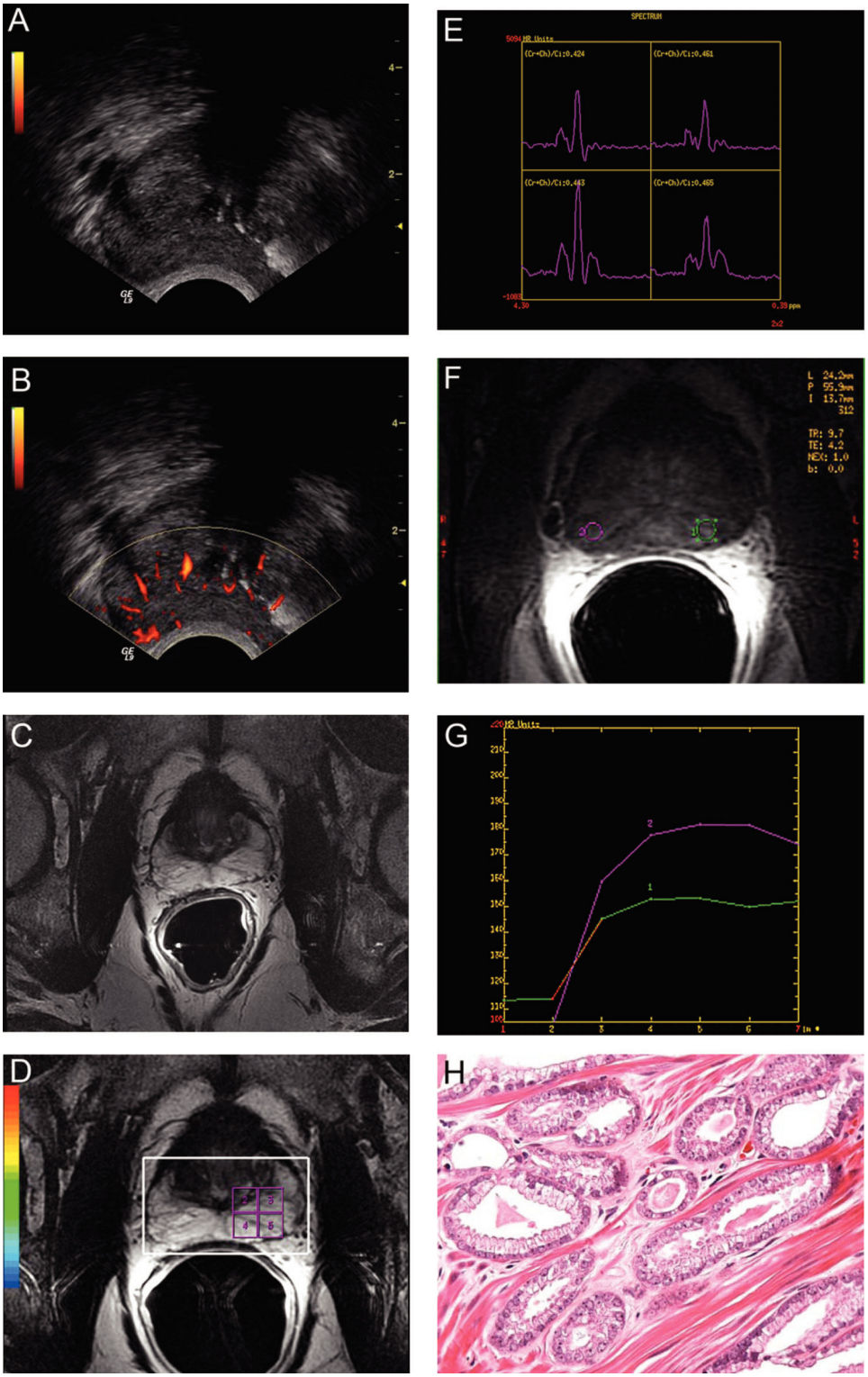

Figure 2 - 68-year-old man with prostate cancer (prostate-specific antigen (PSA) level 2.6 ng/ml). (a) Transverse transrectal ultrasound (TRUS) and amplitude Doppler ultrasound (ADUS) (b) do not demonstrate any suspect finding in the peripheral zone. Transverse T2W MRI (c) shows normal high-signal intensity in the peripheral zone, except for discrete ill-defined areas of hypointensity. Four contiguous voxels in the left prostate mid-gland/apex (d) and the corresponding amplitude times frequency spectroscopic graphic (e) shows normal metabolites concentrations, with low choline and increased citrate levels. Transverse T1W DCE-MRI (f) demonstrates normal hypovascularized peripheral zone in both sides (pink and green ROIs), characterized on graphic (g) by steady state enhancement pattern. Surgically confirmed adenocarcinoma Gleason score 6 (3 + 3) in the in the left base, mid-gland and apex – HE 400× (h).

Although not directly focused on the low-risk group, the mean PSA level of 5.9 ng/dl found in that study may be because that population was skewed toward low-risk and low-volume cancers. Another study evaluated the accuracy of MRI in predicting organ-confined prostate cancer with and without MRS, and found that although the radiologists' performance was slightly higher with combined MRS this difference was not considered statistically significant.[16] Similarly, the addition of MRS did not improve the ability to localize cancers in our study.

Few studies have been performed for evaluating the role of MRI contrast agents in prostate cancer detection. A recent one showed that DCE-MRI was more sensitive than MRI for tumor localization (50% × 21%) without lacking specificity (85% × 81%).[17] In our study, MRI and DCE-MRI showed similar sensitivities (71.5% and 67.2%, respectively), and DCE-MRI allowed an increment in specificity from 58.9% to 65.7%. Once again, the low-volume, low-aggressive tumors in our study group might have impaired the imaging results.

A large literature variation also exists in the local staging performance of prostate MRI, as demonstrated by a large meta-analysis, in part due to the lack of definitive criteria standardization for ECE and to the variability among the studied populations.[18] Different studies in which MRI was used for prostate cancer staging and/or prediction of ECE have yielded a range of values for sensitivity (51–89%), specificity (68–87%) and accuracy (56–88%).[8] One study that evaluated MRI for ECE based on positivity criteria similar to ours obtained sensitivity, specificity, PPV, and NPV of 42.2%, 95.4%, 74.5%, and 83.8%, respectively.[19] However, that study included patients with presurgical Gleason scores ranging from 5 to 10. Although our study presented higher sensitivity and NPV (50% and 95.6%, respectively), we had significantly lower specificity and PPV, which may be explained by the differences in the selected patient group (presurgical Gleason score $\leq$6).

We included TRUS and ADUS in this evaluation because of their higher availability in many centers, associated with lower costs than MRI. TRUS is considered to have poor accuracy for prostate cancer identification and staging in the literature, even with ADUS technical improvements.[20] In spite of that, TRUS and particularly ADUS presented results similar to those of MRI in the present study. Such results may be attributed to specific imaging characteristics of this low-risk cancer population, in which MRI has poor accuracy.

Our study has some limitations. First, we do not have data about the number of biopsy cores or its positive percentual score, as we only had access to the biopsy Gleason score in the patients' medical records. Although our Gleason biopsy understaging rate of 62.9% was slightly high, it does not differ substantially from the available literature. Some studies compared the correlation between Gleason scores of needle biopsies and radical prostatectomy specimens, with biopsy Gleason understaging varying from 38% to 71.7%.[21–25] This relatively low level of agreement was predominantly due to the undergrading of low-grade carcinoma in needle biopsies, although the agreement was more exact in high-grade carcinoma, as described by Lotan and Epstein.[26]

Also, we included a relatively small number of patients and, as expected for a clinically defined low-risk group, our positive histology rate for EPE was small, with considerable impact on our final statistical results. Moreover, only three patients presented with SVI, with a consequent overestimation of the false-negative results and an important repercussion in the sensitivity value. Additionally, as only one reader evaluated each method (TRUS and MRI), we could not assess interobserver variability.

CONCLUSION

Our preliminary results suggest that MRI using different functional sequences and techniques, TRUS and ADUS have limited usefulness in evaluating low-risk prostate cancer.

REFERENCES

1. O'Donnell H, Parker C. What is low-risk prostate cancer and what is its natural history? World J Urol. 2008;26:415–22.
2. Damber JE, Aus G. Prostate cancer. Lancet. 2008;371:1710–21, doi: 10.1016/S0140-6736(08)60729-1.
3. Sartor AO, Hricak H, Wheeler TM, Coleman J, Penson DF, Carroll PR, et al. Evaluating localized prostate cancer and identifying candidates for focal therapy. Urology. 2008;72(6 Suppl):12–24, doi: 10.1016/j.urology.2008.10.004.
4. Cooperberg MR, Lubeck DP, Meng MV, Mehta SS, Carrol PR. The changing face of low-risk prostate cancer: trends in clinical presentation and primary management. J Clin Oncol. 2004;22:2141–9, doi: 10.1200/JCO.2004.10.062.
5. D'Amico AV, Whittington R, Malkowicz SB, Schultz D, Blank K, Broderick GA, et al. Biochemical outcome after radical prostatectomy, external beam radiation therapy, or interstitial radiation therapy for clinically localized prostate cancer. JAMA. 1998;280:969–74, doi: 10.1001/jama.280.11.969.
6. Steyerberg EW, Roobol MJ, Kattan MW, van der Kwast TH, Koning HJ, Schröder FH. Prediction of indolent prostate cancer: validation and updating of a prognostic nomogram. J Urol. 2007; 177:107–12.
7. Shukla-Dave A, Hricak H and Scardino PT. Imaging low-risk prostate cancer. Curr Opin Urol. 2008;18:78–86, doi: 10.1097/MOU.0b013e3282f13adc.
8. Bloch BN, Furman-Haran E, Helbich TH, Lenkinski RE, Degani H, Kratzik C, et al. Prostate cancer: accurate determination of extracapsular extension with high-spatial-resolution dynamic contrast-enhanced and T2-weighted MR imaging-initial results. Radiology. 2007;245:176–85, doi: 10.1148/radiol.2451061502.
9. Yu KK, Hricak H, Alagappan R, Chernoff DM, Bacchetti P, Zaloudek CJ. Detection of extracapsular extension of prostate carcinoma with endorectal and phased-array coil MR imaging: multivariate feature analysis. Radiology. 1997;202:697–702.
10. Sala E, Akin O, Moskowitz CS, Eisenberg HF, Kuroiwa K, Ishill NM, et al. Endorectal MR imaging in the evaluation of seminal vesicle invasion: diagnostic accuracy and multivariate feature analysis. Radiology. 2006;238:929–37, doi: 10.1148/radiol.2383050657.
11. Jung JA, Coakley FV, Vigneron DB, Swanson MG, Qayyum A, Weinberg V, et al. Prostate depiction at endorectal MR spectroscopic imaging: investigation of a standardized evaluation system. Radiology. 2004;33:701–8, doi: 10.1148/radiol.2333030672.
12. Harnden P, Naylor B, Shelley MD, Clements H, Coles B, Mason MD. The clinical management of patients with a small volume of prostatic cancer on biopsy: what are the risks of progression? A systematic review and meta-analysis. Cancer. 2008;112:971–81, doi: 10.1002/cncr.23277.
13. Kirkham AP, Emberton M, Allen C. How good is MRI at detecting and characterising cancer within the prostate? Eur Urol. 2006; 50:1163–74, doi: 10.1016/j.eururo.2006.06.025.
14. Westphalen AC, Coakley FV, Qayyum A, Swanson M, Simko JP, Lu Y, et al. Peripheral zone prostate cancer: accuracy of different interpretative approaches with MR and MR spectroscopic imaging. Radiology. 2008; 246:177–84, doi: 10.1148/radiol.2453062042.
15. Weinreb JC, Blume JD, Coakley FV, Wheeler TM, Cormack JB, Sotto CK, et al. Prostate Cancer: Sextant Localization at MR Imaging and MR Spectroscopic Imaging before Prostatectomy - Results of ACRIN Prospective Multi-institutional Clinicopathologic Study. Radiology. 2009;251:122–33, doi: 10.1148/radiol.2511080409.
16. Wang L, Hricak H, Kattan MW, Chen HN, Scardino PT, Kuroiwa K. Prediction of Organ-confined Prostate Cancer: Incremental Value of MR Imaging and MR Spectroscopic Imaging to Staging Nomograms. Radiology. 2006;238:597–603, doi: 10.1148/radiol.2382041905.
17. Jackson ASN, Reinsberg SA, Sohaib SA, Charles-Edward EM, Jhavar S, Christmas TJ. Dynamic contrast-enhanced MRI for prostate cancer localization. Br J Radiol. 2009;82:148–56.

18. Engelbrecht MR, Jager GJ, Laheij RJ, Verbeek ALM, van Lier HJ, Barentsz JO. Local staging of prostate cancer using magnetic resonance imaging: a meta-analysis. Eur Radiol. 2002;12:2294–302.
19. Wang L, Mullerad M, Chen HN, Eberhardt SC, Kattan MW, Scardino PT, et al: Prostate Cancer: incremental value of endorectal MR imaging findings for prediction of extracapsular extension. Radiology. 2004;232:133–9, doi: 10.1148/radiol.2321031086.
20. Puech P, Huglo D, Petyt G, Lemaitre L, Villers A. Imaging of organ-confined prostate cancer: functional ultrasound, MRI and PET/computed tomography. Curr Opin Urol. 2009;19:168–76, doi: 10.1097/MOU.0b013e328323f5ed.
21. Cookson MS, Fleshner NE, Soloway SM, Fair WR. Correlation between Gleason score of needle biopsy and radical prostatectomy specimen: accuracy and clinical implications. J Urol. 1997;157:559–62.
22. Djavan B, Kadesky K, Klopukh B, Marberger M, Roehrborn CG. Gleason scores from prostate biopsies obtained with 18-gauge biopsy needles poorly predict Gleason scores of radical prostatectomy specimens. Eur Urol. 1998;33:261–70, doi: 10.1159/000019578.
23. Kvale R, Moller B, Wahlqvist R, Fossa SD, Berner A, Busch C, et al. Concordance between Gleason scores of needle biopsies and radical prostatectomy specimens: a population-based study. BJU Int. 2009;103: 1647–54, doi: 10.1111/j.1464-410X.2008.08255.x.
24. Köksal IT, Ozcan F, Kadioglu TC, Esen T, Kiliçaslan I, Tunç M. Discrepancy between Gleason scores of biopsy and radical prostatectomy specimens. Eur Urol. 2000;37:670–4, doi: 10.1159/000020216.
25. Cam K, Yucel S, Turkeri L, Akdas A. Accuracy of transrectal ultrasound guided prostate biopsy: histopathological correlation to matched prostatectomy specimens. Int J Urol. 2002;9:257–60.
26. Lotan TL, Epstein JI. Clinical implications of changing definitions within the Gleason grading system. Nat. Rev. Urol. 2010;7:136–42, doi: 10.1038/nrurol.2010.9.